Inorganic Chemistry

Article

pubs.acs.org/IC

Role of Hydrogen-Bonding in the Formation of Polar Achiral and Nonpolar Chiral Vanadium Selenite Frameworks

Jacob H. Olshansky,[†] Thanh Thao Tran,[‡] Kristen J. Hernandez,[§] Matthias Zeller,[§] P. Shiv Halasyamani,[‡] Joshua Schrier,[†] and Alexander J. Norquist*,[†]

[†]Department of Chemistry, Haverford College, 370 Lancaster Avenue, Haverford, Pennsylvania 19041, United States

[‡]Department of Chemistry, University of Houston, Houston, Texas 77204, United States

[§]Department of Chemistry, Youngstown State University, Youngstown, Ohio 44555, United States

Supporting Information

ABSTRACT: A series of organically templated vanadium selenites have been prepared under mild hydrothermal conditions. Single crystals were grown from mixtures of $VOSO_4$, SeO_2, and either 1,4-dimethylpiperazine, 2,5-dimethylpiperazine, or 2-methylpiperazine in H_2O. Each compound contains one-dimensional $[VO(SeO_3)(HSeO_3)]_n^{n-}$ secondary building units, which connect to form three-dimensional frameworks in the presence of 2,5-dimethylpiperazine or 2-methylpiperazine. Differences in composition and both *intra*-secondary building unit and organic–inorganic hydrogen-bonding between compounds dictate the dimensionality of the resulting inorganic structures. [1,4-dimethylpiperazineH_2]-$[VO(SeO_3)(HSeO_3)]_2$ contains one-dimensional $[VO(SeO_3)(HSeO_3)]_n^{n-}$ chains, while [2,5-dimethylpiperazineH_2]$[VO(SeO_3)(HSeO_3)]_2\cdot 2H_2O$ contains a three-dimensional $[VO(SeO_3)(HSeO_3)]_n^{n-}$ framework. The use of racemic 2-methylpiperazine also results in a compound containing a three-dimensional $[VO(SeO_3)(HSeO_3)]_n^{n-}$ framework, crystallizing in the noncentrosymmetric polar, achiral space group $Pca2_1$ (no. 29), while analogous reactions containing either (*R*)-2-methylpiperazine or (*S*)-2-methylpiperazine result in noncentrosymmetric, nonpolar chiral frameworks that crystallize in $P2_12_12$ (no. 18). The formation of these noncentrosymmetric framework materials is dictated by the structure, symmetry, and hydrogen-bonding properties of the [2-methylpiperazineH_2]$^{2+}$ cations.

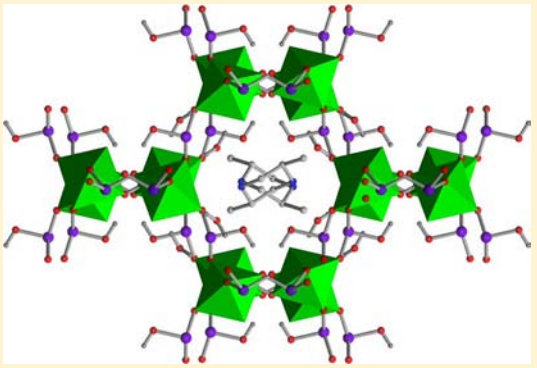

INTRODUCTION

The formation of either open-framework or noncentrosymmetric materials has been the focus of intense interest for many years, owing to the wide range of desirable physical properties that these two classes of compounds can exhibit.[1,2] The combination of both an open-framework *and* noncentrosymmetry within a single compound is especially attractive, with notable examples including zeolites,[3,4] copper phosphates,[5] chalcohalides,[6] oxo-thioantimonates,[7] and homochiral metal organic frameworks.[8,9] However, strategies used for synthesizing framework and noncentrosymmetric materials differ greatly. New noncentrosymmetric materials are often prepared using asymmetric building units,[10−16] such as second−order Jahn−Teller active cations,[17−19] or transition-metal oxide fluorides.[20−23] The formation of open-framework metal oxo compounds has also been discussed in great detail in the context of a wide range of systems.[1,24,25] Rao, Cheetham, and Ferey,[26,27] among others,[28] have highlighted the importance of metal oxo secondary building units and organic amines in the formation of such compounds.[27,29−31]

Templated vanadium tellurites and selenites represent attractive systems for study, owing to the presence of multiple asymmetric building units, including the possibility of chiral organic amines, out-of-center octahedral distortions on vanadium cations, and stereoactive lone pairs on the Te^{4+} and Se^{4+} centers. Within the small number of reported templated vanadium tellurites,[32−39] both framework[39] and noncentrosymmetric compounds are observed.[37] However, neither noncentrosymmetric nor framework structures have been reported in templated vanadium selenites.[32−39] Yet, templated vanadium selenites represent particularly interesting because the much higher water solubility of SeO_2 versus TeO_2 suggests the promise of wider structural and compositional flexibility with respect to templated tellurites.

A series of new organically templated vanadium selenites are reported, including the centrosymmetric compounds $[C_6H_{16}N_2][VO(SeO_3)(HSeO_3)]_2$ (**1**) and $[C_6H_{16}N_2][VO(SeO_3)(HSeO_3)]_2\cdot 2H_2O$ (**2**) and the noncentrosymmetric compounds $[C_5H_{14}N_2][VO(SeO_3)(HSeO_3)]_2\cdot 2H_2O$ (**3**), $[(R)\text{-}C_5H_{14}N_2][VO(SeO_3)(HSeO_3)]_2\cdot 2H_2O$ (**4a**), and $[(S)\text{-}C_5H_{14}N_2][VO(SeO_3)(HSeO_3)]_2\cdot 2H_2O$ (**4b**). Compounds **2**, **3**,

Received: July 16, 2012
Published: September 24, 2012

Table 1. Crystallographic Data for Compounds 1, 2, 3, 4a, and 4b

compound	$[C_6H_{16}N_2][VO(SeO_3)(HSeO_3)]_2$ (1)	$[C_6H_{16}N_2][VO(SeO_3)(HSeO_3)]_2{\cdot}2H_2O$ (2)	$[C_5H_{14}N_2][VO(SeO_3)(HSeO_3)]_2{\cdot}2H_2O$ (3)	$[(R)\text{-}C_5H_{14}N_2][VO(SeO_3)(HSeO_3)]_2{\cdot}2H_2O$ (4a)	$[(S)\text{-}C_5H_{14}N_2][VO(SeO_3)(HSeO_3)]_2{\cdot}2H_2O$ (4b)
formula	$C_6H_{18}N_2O_{14}Se_4V_2$	$C_6H_{22}N_2O_{16}Se_4V_2$	$C_5H_{20}N_2O_{16}Se_4V_2$	$C_5H_{20}N_2O_{16}Se_4V_2$	$C_5H_{20}N_2O_{16}Se_4V_2$
fw	759.94	795.97	781.94	781.94	781.94
space group	$P2_1/c$ (no. 14)	$Pbcn$ (no. 60)	$Pca2_1$ (no. 29)	$P2_12_12$ (no. 18)	$P2_12_12$ (no. 18)
a/Å	9.903(4)	14.5262(15)	10.523(5)	14.419(2)	14.411(3)
b/Å	6.077(2)	10.6006(11)	14.283(5)	12.682(2)	12.674(2)
c/Å	18.013(6)	12.7160(14)	12.667(5)	10.5365(17)	10.539(2)
β/°	121.916(5)	90	90	90	90
V/Å^3	920.2(6)	1958.1(4)	1917.0(14)	1926.7(5)	1924.8(7)
Z	2	4	4	4	4
ρ_{calc}/g cm^{-3}	2.743	2.700	2.709	2.695	2.698
λ/Å	0.71073	0.71073	0.71073	0.71073	0.71073
T/K	100(2)	100(2)	100(2)	100(2)	100(2)
μ/mm^{-1}	9.002	8.474	8.653	8.609	8.618
Flack parameter	-	-	0.199(11)	0.027(11)	0.026(12)
R_1[a]	0.0361	0.0157	0.0192	0.0236	0.0241
wR_2[b]	0.0834	0.0381	0.0447	0.0642	0.0604

[a] $R_1 = \sum||F_o| - |F_c||/\sum|F_o|$. [b] $wR_2 = [\sum w(F_o^2 - F_c^2)^2/[\sum w(F_o^2)^2]^{1/2}$.

and **4a**/**4b** constitute the first organically templated vanadium selenites with three-dimensional frameworks. Within these compounds, we observe centrosymmetric (**2**), polar-achiral (**3**), and nonpolar-chiral (**4a**/**4b**) framework structures. Moreover, the roles of composition, hydrogen-bonding, and amine chirality are shown to be integral to the dimensionality and symmetry of the inorganic components of these compounds.

EXPERIMENTAL SECTION

Materials. $VOSO_4$ (97%), 1,4-dimethylpiperazine (1,4-dmpip, 98%), and 2-methylpiperazine (2-mpip, 95%) were purchased from Sigma-Aldrich. SeO_2 (99.4%), *trans*-2,5-dimethylpiperazine (2,5-dmpip, 98%), (*S*)-(+)-2-methylpiperazine ((*S*)-2-mpip, 98+ %), and (*R*)-(-)-2-methylpiperazine ((*R*)-2-mpip, 98+ %) were purchased from Alfa Aesar. All reagents were used as received. Deionized water was used in these syntheses.

Synthesis. All reactions were conducted in 23 mL poly(fluoroethylene-propylene) lined pressure vessels and contained a 1:12:1 ratio of $VOSO_4$:SeO_2:amine with 6 mL of H_2O. The pH of each reaction mixture was adjusted to 2 upon the addition of 0.5 mL of 4 M NaOH. Reaction mixtures were stirred for 30 s with a glass rod before being placed into pressure vessels and heated to either 90 or 110 °C for 24 h, followed by a slow cooling to room temperature at a rate of 6 °C h^{-1}. The pressure vessels were opened in air, and products were recovered through vacuum filtration. Postreaction pH values ranged between 1 and 2.

$[C_6H_{16}N_2][VO(SeO_3)(HSeO_3)]_2$ (**1**) was synthesized through the reaction of 0.1650 g (1.01×10^{-3} mol) of $VOSO_4$, 1.335 g (1.20×10^{-2} mol) of SeO_2, 0.1155 g (1.01×10^{-3} mol) of 1,4-dmpip, and 6.0056 g (0.333 mol) of deionized water at 90 °C. Blue rods were recovered in 35% yield, based upon vanadium. Elemental microanalysis for **1** obsd (calc): C 9.40 (9.48), H 2.16 (2.39), N 3.56 (3.69), V 12.80 (13.41), Se 39.33 (41.56). IR data: O−H 3447 cm^{-1}, C−H 3044 cm^{-1}, N−H 1644, 1531, 1459 cm^{-1}, V═O 992 cm^{-1}, Se−O 820 cm^{-1}.

$[C_6H_{16}N_2][VO(SeO_3)(HSeO_3)]_2{\cdot}2H_2O$ (**2**) was synthesized through the reaction of 0.1644 g (1.01×10^{-3} mol) of $VOSO_4$, 1.3602 g (1.23×10^{-2} mol) of SeO_2, 0.1220 g (1.07×10^{-3} mol) of 2,5-dmpip, and 6.0416 g (0.335 mol) of deionized water at 90 °C. Aquamarine blocks were recovered in 66% yield, based upon vanadium. Elemental microanalysis for **2** obsd (calc): C 9.06 (9.05), H 2.67 (2.79), N 3.54 (3.52), V 13.27 (12.80), Se 37.75 (39.68). IR data: O−H 3251 cm^{-1}, N−H 1639, 1469, 1442 cm^{-1}, V═O 958 cm^{-1}, Se−O 806 cm^{-1}.

$[C_5H_{14}N_2][VO(SeO_3)(HSeO_3)]_2{\cdot}2H_2O$ (**3**) was synthesized through the reaction of 0.1634 g (1.00×10^{-3} mol) of $VOSO_4$, 1.3052 g (1.18×10^{-2} mol) of SeO_2, 0.1099 g (1.10×10^{-3} mol) of 2-mpip, and 6.0423 g (0.335 mol) of deionized water at 110 °C. Aquamarine blocks were recovered in 33% yield, based upon vanadium. Elemental microanalysis for **3** obsd (calc): C 7.71 (7.68), H 2.38 (2.58), N 3.49 (3.58), V 13.07 (13.03), Se 39.64 (40.39). IR data: O−H 3247 cm^{-1}, N−H 1686, 1637, 1487 cm^{-1}, V═O 963 cm^{-1}.

$[(R)\text{-}C_5H_{14}N_2][VO(SeO_3)(HSeO_3)]_2{\cdot}2H_2O$ (**4a**) was synthesized through the reaction of 0.1636 g (1.00×10^{-3} mol) of $VOSO_4$, 1.3203 g (1.19×10^{-2} mol) of SeO_2, 0.1074 g (1.07×10^{-3} mol) of (*R*)-2-mpip, and 6.6555 g (0.369 mol) of deionized water at 110 °C. Aquamarine blocks were recovered in 32% yield, based upon vanadium. Elemental microanalysis for **4a** obsd (calc): C 7.69 (7.68), H 2.44 (2.58), N 3.50 (3.58), V 12.58 (13.03), Se 38.53 (40.39). IR data: O−H 3238 cm^{-1}, N−H 1686, 1637, 1490 cm^{-1}, V═O 958 cm^{-1}, Se−O 811 cm^{-1}.

$[(S)\text{-}C_5H_{14}N_2][VO(SeO_3)(HSeO_3)]_2{\cdot}2H_2O$ (**4b**) was synthesized through the reaction of 0.1636 g (1.00×10^{-3} mol) of $VOSO_4$, 1.3245 g (1.19×10^{-2} mol) of SeO_2, 0.1203 g (1.20×10^{-3} mol) of (*S*)-2-mpip and 5.7953 g (0.322 mol) of deionized water at 110 °C. Aquamarine blocks were recovered in 33% yield, based upon vanadium. Elemental microanalysis for **4b** obsd (calc): C 7.71 (7.68), H 2.44 (2.58), N 3.53 (3.58), V 12.94 (13.03), Se 39.74 (40.39). IR data: O−H 3238 cm^{-1}, N−H 1686, 1637, 1490 cm^{-1}, V═O 958 cm^{-1}, Se−O 811 cm^{-1}.

Single Crystal X-ray Diffraction. Data were collected using a Bruker AXS Smart Apex CCD diffractometer with Mo−Kα radiation (λ = 0.71073 Å). Single crystals were mounted on a Mitegen micromesh mount using a trace of mineral oil and cooled *in situ* to 100(2) K for data collection. Frames were collected, indexed, and processed, and the files were scaled and corrected for absorption using APEX2.[40] The heavy atom positions were determined using SIR92.[41] All other non-hydrogen sites were located from Fourier difference maps. All non-hydrogen sites were refined using anisotropic thermal parameters using full matrix least-squares procedures on F_o^2 with $I > 3\sigma(I)$. Hydrogen atoms attached to $[HSeO_3]$ groups and H_2O molecules were located from difference maps, and the X−H bond lengths were normalized. Organic ammonium cation hydrogen atoms were placed in geometrically idealized positions. All calculations were performed using Crystals.[42] Relevant crystallographic data are listed in Table 1.

Powder X-ray Diffraction. Powder diffraction patterns were recorded on a GBC-Difftech MMA powder diffractometer. Samples

dx.doi.org/10.1021/ic3015496 | Inorg. Chem. 2012, 51, 11040−11048

were mounted on aluminum plates. Calculated powder patterns were generated from single crystal data using ATOMS *v*. 6.0.[43] Bulk powder diffraction patterns for each compound matched calculated patterns, indicating relative phase purity.

Infrared Spectroscopy. Infrared measurements were obtained using a Perkin-Elmer FT-IR Spectrum 1000 spectrophotometer. Samples were diluted with spectroscopic grade KBr and pressed into pellets. Scans were run over the range of 400−4000 cm^{-1}.

Thermogravimetric Analysis. Thermogravimetric analyses (TGA) were conducted using a Q500 thermogravimetric analyzer from TA Instruments. Samples were contained within a platinum crucible and heated under flowing nitrogen at 10 °C min^{-1} to 950 °C. TGA traces are available in the Supporting Information.

Second Harmonic Generation. Powder SHG measurements were conducted using a modified Kurtz−NLO system, with a 1064 nm light source.[44,45] Polycrystalline $[C_5H_{14}N_2][VO(SeO_3)(HSeO_3)]_2{\cdot}2H_2O$ (**3**), $[(R)\text{-}C_5H_{14}N_2][VO(SeO_3)(HSeO_3)]_2{\cdot}2H_2O$ (**4a**), and $[(S)\text{-}C_5H_{14}N_2][VO(SeO_3)(HSeO_3)]_2{\cdot}2H_2O$ (**4b**) were ground and sieved into distinct particle size ranges: <20 μm, 20−45 μm, 45−63 μm, 63−75 μm, 75−90 μm, and 90−120 μm. Crystalline α-SiO_2 was ground and sieved into identical particle size ranges in order to compare the SHG properties of compounds **3** and **4a**/**4b** to known materials. All powders were placed in separate capillary tubes, no index-matching fluid was used in any experiment. The SHG, i.e. 532 nm light, was collected in reflection mode and detected using a photomultiplier tube. A 532 nm narrow−bandpass interference filter was attached to the tube in order to detect the SHG light only.

Electronic Structure Calculations. Solid-state electronic structure calculations were performed using ABINIT *v*6.4.1 and *v*6.12.1,[46,47] using the Perdew-Burke-Ernzerhof generalized gradient approximation (PBE-GGA) exchange-correlation functional, norm-conserving Troullier-Martins pseudopotentials, a planewave basis set with energy cutoff of 35 hartrees, and utilizing the experimental crystal structures. Sampling of the Brillouin zone was performed with a 6 × 6 × 6 Monkhorst-Pack grid.

Electron Localization Function (ELF). ELFs were computed from the self-consistent valence electron density. ELFs were visualized using Vesta *v*1.1.0[48] with an isosurface value of 0.96.

Partial Charges and Dipole Moments. Iterative Hirshfeld (Hirshfeld-I)[49,50] atomic partial charge determinations were performed on the self-consistent valence electron density in conjunction with all-electron atomic charge densities generated using the HF96 atomic Hartree−Fock code,[51] as described in our previous work.[37] Full tables of partial atomic charges for **2** and **3** are provided in the Supporting Information. Dipole moments were calculated from the partial charges and atomic positions using a methodology described earlier.[15,20,37,52]

Bond Valence Sums. Oxidation states were verified and hydrogen-bonding networks were analyzed using bond valence sums,[53] with parameters compiled by Brese and O'Keeffe.[54] The valences of O−H bonds are approximated as 0.8.[55] Complete bond valence sums for compounds **1**, **2**, **3**, and **4a**/**4b** are available in the Supporting Information.

RESULTS AND DISCUSSION

The inorganic components in compounds **1**, **2**, **3**, **4a**, and **4b**, all share the formula $[VO(SeO_3)(HSeO_3)]_n^{n-}$. In compound **1**, the vanadium(IV) sites are five-coordinate with a $V{-}O_{terminal}$ bond of 1.593(4) Å and $V{-}O_{bridging}$ bonds that range between 1.990(3) and 2.023(3) Å. In compounds **2**, **3**, **4a**, and **4b**, all vanadium(IV) centers have distorted octahedral geometries. The $V{-}O_{terminal}$ bonds range between 1.604(3) and 1.615(3) Å, the $V{-}O_{equatorial}$ bonds range between 2.004(4) and 2.0600(11) Å, and the $V{-}O_{trans}$ bonds range between 2.226(3) and 2.404(11) Å. The selenium sites in all compounds reported here are 4+ and exhibit a trigonal pyramidal geometry with a stereoactive lone pair. All compounds contain both unprotonated $[SeO_3]$ and protonated $[HSeO_3]$ moieties. The $Se{-}O_{bridging}$ bonds range between 1.675(3) and 1.720(3) Å, and Se−O(H) bonds range between 1.758(3) Å and 1.774(3). In compound **1**, there is also a $Se{-}O_{terminal}$ bond with a length of 1.670(4) Å. The bond valence sums for vanadium and selenium sites range between 3.93 and 4.02 and between 3.86 and 4.03, respectively. Complete tables of bond lengths and angles can be found in .cif format in the Supporting Information.

$[C_6H_{16}N_2][VO(SeO_3)(HSeO_3)]_2$ (**1**) contains an inorganic chain with a backbone composed of $[VO_5]$ and $[SeO_3]$ groups linked in an alternating ladder pattern. See Figure 1. An *intra*-chain hydrogen bond is formed between $[HSeO_3]$ groups and O4, as seen in Figure 1. The chains align in pseudolayers, between which $[1,4\text{-dmpip}H_2]^{2+}$ cations reside. Hydrogen bonds are observed between $[1,4\text{-dmpip}H_2]^{2+}$ cations and the terminal oxygen (O7) of the $[HSeO_3]$ group. $[C_6H_{16}N_2][VO(SeO_3)(HSeO_3)]_2{\cdot}2H_2O$ (**2**), $[C_5H_{14}N_2][VO(SeO_3)(HSeO_3)]_2{\cdot}2H_2O$ (**3**), $[(R)\text{-}C_5H_{14}N_2][VO(SeO_3)(HSeO_3)]_2{\cdot}2H_2O$ (**4a**), and $[(S)\text{-}C_5H_{14}N_2][VO(SeO_3)(HSeO_3)]_2{\cdot}2H_2O$ (**4b**) are the first reported organically templated vanadium selenites with three-dimensional inorganic frameworks. See Figure 2. These frameworks are constructed from chains that are similar to those observed in **1**. However, the terminal oxygen atoms on the pendant $[HSeO_3]$ moieties link to vanadium atoms on neighboring chains, which results in a three-dimensional inorganic structure.

The inorganic components in **1**, **2**, **3**, and **4a**/**4b** are constructed from essentially the same one-dimensional secondary building units (SBUs). These ladder-type chains have also been observed in other vanadium selenites, including $[C_4H_{12}N_2][VO(H_2O)_2(SeO_3)]_2[SO_4]$,[56] $[[VO(H_2O)_2](SeO_3)]_4{\cdot}2H_2O$,[57] $[C_4H_{12}N_2]_{0.5}[(VO)_2(H_2O)_2(SeO_3)_2(HSeO_3)]$,[58] and $[C_6H_{14}N_2][VO(SeO_3)(HSeO_3)]_2{\cdot}2H_2O$.[59] In fact, analogous ladder-type SBU chains have been shown to be an important building unit in zinc phosphates,[60] in which these low-dimensional SBUs participate in processes by which higher-dimensionality structures are constructed.[24,61]

Despite the presence of ladder-type SBUs in **1**, **2**, **3**, **4a**/**4b**, $[C_4H_{12}N_2][VO(H_2O)_2(SeO_3)]_2[SO_4]$, $[[VO(H_2O)_2](SeO_3)]_4{\cdot}2H_2O$, $[C_4H_{12}N_2]_{0.5}[(VO)_2(H_2O)_2(SeO_3)_2(HSeO_3)]$,[58] and $[C_6H_{14}N_2][VO(SeO_3)(HSeO_3)]_2{\cdot}2H_2O$, differences in the structures and compositions of the inorganic components in these compounds exist.

The difference in composition between **1**, **2**, $[C_6H_{14}N_2][VO(SeO_3)(HSeO_3)]_2{\cdot}2H_2O$,[59] $[C_4H_{12}N_2][VO(H_2O)_2(SeO_3)]_2[SO_4]$,[56] and $[C_4H_{12}N_2]_{0.5}[(VO)_2(H_2O)_2(SeO_3)_2(HSeO_3)]$[58] is dictated by the reactant concentrations in the mixtures from which these compounds were synthesized.[62−65] Compounds **1**, **2**, and $[C_6H_{14}N_2][VO(SeO_3)(HSeO_3)]_2{\cdot}2H_2O$[59] were all synthesized from reaction mixtures in which the V:Se:amine ratios were fixed at 1:12:1, while $[C_4H_{12}N_2][VO(H_2O)_2(SeO_3)]_2[SO_4]$[56] and $[C_4H_{12}N_2]_{0.5}[(VO)_2(H_2O)_2(SeO_3)_2(HSeO_3)]$[58] were synthesized from reaction mixtures with compositions of 1:3:1 and 1:2.5:2, respectively. Consequently, the 'selenium rich' conditions under which **1**, **2**, and $[C_6H_{14}N_2][VO(SeO_3)(HSeO_3)]_2{\cdot}2H_2O$ were synthesized are mirrored in their respective compositions, and each compound has a 1:2 vanadium to selenium ratio. The 'selenium deficient' conditions used for the preparation of $[C_4H_{12}N_2][VO(H_2O)_2(SeO_3)]_2[SO_4]$ and $[C_4H_{12}N_2]_{0.5}[(VO)_2(H_2O)_2(SeO_3)_2(HSeO_3)]$ resulted in compounds that incorporated fewer $[SeO_3]$ groups per vanadium center, with either a 1:1 or a 2:3 vanadium to selenium ratio.

The inorganic layers in $[C_6H_{14}N_2][VO(SeO_3)(HSeO_3)]_2{\cdot}2H_2O$[59] are constructed through links between

dx.doi.org/10.1021/ic3015496 | *Inorg. Chem.* 2012, 51, 11040−11048

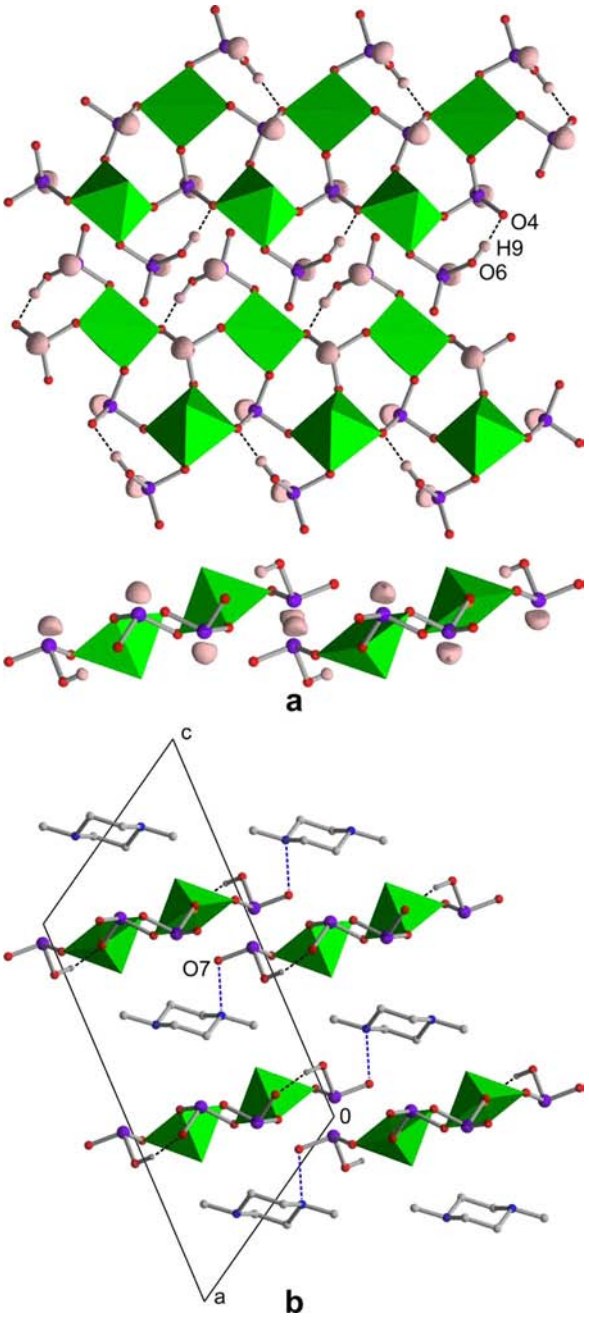

Figure 1. (a) Two views of the $[VO(SeO_3)(HSeO_3)]_n^{n-}$ chains with ELF isosurfaces shown with a boundary condition of 0.96 and (b) the three-dimensional packing of $[C_6H_{16}N_2][VO(SeO_3)(HSeO_3)]_2$ (**1**). Green polyhedra represent $[VO_5]$, while purple, red, blue, white, and gray spheres represent selenium, oxygen, nitrogen, carbon, and hydrogen, respectively. Selected hydrogen-bonding interactions are shown as dashed lines. Organic ammonium cation hydrogen atoms have been removed for clarity.

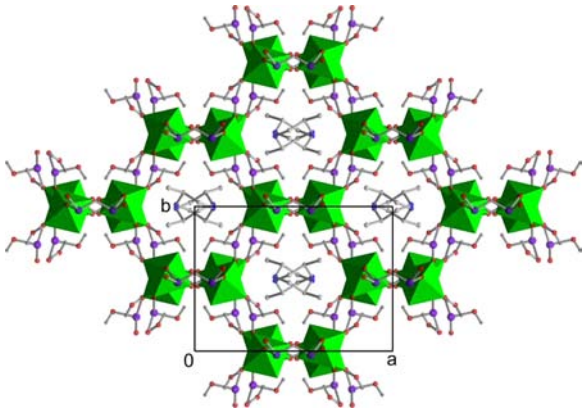

Figure 2. Three-dimensional packing of $[C_6H_{16}N_2][VO(SeO_3)(HSeO_3)]_2{\cdot}2H_2O$ (**2**). Green polyhedra represent $[VO_6]$, while purple, red, blue, white, and gray spheres represent selenium, oxygen, nitrogen, carbon, and hydrogen, respectively. Organic ammonium cation hydrogen atoms have been removed for clarity.

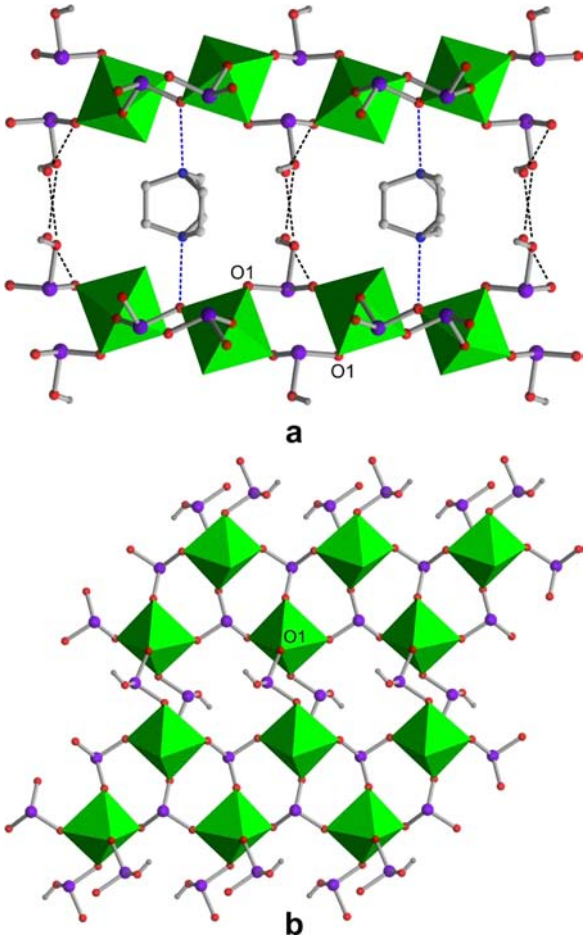

Figure 3. (a) Hydrogen-bonding interactions, shown as dashed lines, and (b) $[VO(SeO_3)(HSeO_3)]_n^{n-}$ layers in $[C_6H_{14}N_2][VO(SeO_3)(HSeO_3)]_2{\cdot}2H_2O$. Green polyhedra represent $[VO_6]$, while purple, red, blue, white, and gray spheres represent selenium, oxygen, nitrogen, carbon, and hydrogen, respectively. Selected hydrogen atoms have been removed for clarity.

pendant $[HSeO_3]$ groups (O1) and vanadium atoms on adjacent chains. See Figure 3. This compound contains $[dabcoH_2]^{2+}$ cations that reside between layers and donate hydrogen bonds to oxide anions on adjacent inorganic layers. A schematic of the formation of the inorganic components from a common SBU chain is shown in Figure 4. Connections between chains are formed via $[HSeO_3]$ groups. The Se–$O_{terminal}$ bonds bridge to adjacent vanadium centers, with these oxide anions occupying the sixth coordination sites in these nearby $[VO_6]$ polyhedra. This process is controlled by the orientation of the $[HSeO_3]$ groups with respect to the one-dimensional SBUs. In order to directly ascribe the differences in structure to the hydrogen-bonding interactions, **1**, $[C_6H_{14}N_2]$-

dx.doi.org/10.1021/ic3015496 | *Inorg. Chem.* 2012, 51, 11040–11048

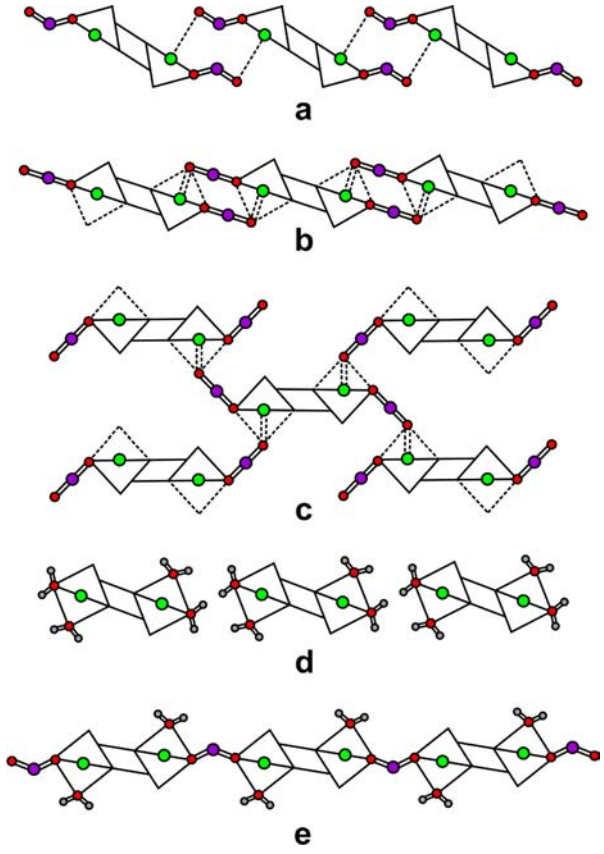

Figure 4. Representation of the formation of inorganic structures in (a) **1**, (b) $[C_6H_{14}N_2][VO(SeO_3)(HSeO_3)]_2{\cdot}2H_2O$, (c) **2**, (d) $[C_4H_{12}N_2][VO(H_2O)_2(SeO_3)]_2[SO_4]$ and $[[VO(H_2O)_2](SeO_3)]_4{\cdot}2H_2O$, and (e) $[C_4H_{12}N_2]_{0.5}[(VO)_2(H_2O)_2(SeO_3)_2(HSeO_3)]$. Green and purple circles represent vanadium and selenium, respectively.

$[VO(SeO_3)(HSeO_3)]_2{\cdot}2H_2O$, and **2** were all synthesized as phase pure samples from reaction mixtures in which the $VOSO_4$:SeO_2:amine ratios were fixed at 1:12:1. The only difference between reactions was the structure of the amine.

In **1**, the orientations of these $[HSeO_3]$ trigonal pyramids directly oppose one another, which precludes close contact between adjacent $[VO(SeO_3)(HSeO_3)]_n^{n-}$ chains. The orientations of the $[HSeO_3]$ groups in **1** are determined by the hydrogen bonds that they donate. In this compound, the only hydrogen bond acceptors are the oxide anions within the inorganic chains. As such, hydrogen-bonding interactions are formed between pendant $[HSeO_3]$ groups and the central chain backbones. The acceptor oxygen atom (O4) is relatively nucleophilic,[66−71] as demonstrated by the bond valence sums shown in the Supporting Information, and the *intra*-chain hydrogen bonds fix the orientations of the $[HSeO_3]$ groups. The steric bulk of the stereoactive lone pairs on the $[HSeO_3]$ groups precludes the $[VO(SeO_3)(HSeO_3)]_n^{n-}$ chains moving closer to one another, as shown in Figure 1a. The distance between V1 and O7, which occupies its 'empty' sixth coordination site, is 2.688(4) Å. The valence of this bond (0.09 vu) falls below the minimal value of a *trans* bond for V^{4+} cation for a [1 + 4 + 1] geometry, as defined by Schindler et al.[72]

Comparison of the structures of **1** and $[C_6H_{14}N_2][VO(SeO_3)(HSeO_3)]_2{\cdot}2H_2O$[59] reveals both strong similarities and differences. The $[1,4\text{-dmpipH}_2]^{2+}$ cations in **1** and the $[dabcoH_2]^{2+}$ cations in $[C_6H_{14}N_2][VO(SeO_3)(HSeO_3)]_2{\cdot}2H_2O$ both donate two hydrogen bonds in a roughly linear fashion. See Figure 1b and Figure 3. However, the 'footprint' of the $[1,4\text{-dmpipH}_2]^{2+}$ cations in **1** is much larger than that of the $[dabcoH_2]^{2+}$ cations in $[C_6H_{14}N_2][VO(SeO_3)(HSeO_3)]_2{\cdot}2H_2O$. The $[1,4\text{-dmpipH}_2]^{2+}$ cations largely occupy the space between layers of $[VO(SeO_3)(HSeO_3)]_n^{n-}$ chains in **1**. In contrast, the $[dabcoH_2]^{2+}$ cations occupy less of the interlayer spacing in $[C_6H_{14}N_2][VO(SeO_3)(HSeO_3)]_2{\cdot}2H_2O$, requiring the inclusion of water molecules to fill the space.

The inclusion of water molecules in $[C_6H_{14}N_2][VO(SeO_3)(HSeO_3)]_2{\cdot}2H_2O$ introduces additional nucleophilic hydrogen bond acceptors, which results in marked differences in the hydrogen-bonding networks. The occluded water molecules are stronger hydrogen bond acceptors than any oxide anion within the inorganic component in $[C_6H_{14}N_2][VO(SeO_3)(HSeO_3)]_2{\cdot}2H_2O$, as determined using bond valence sums. The orientations of the $[HSeO_3]$ groups are dictated by the $O{-}H{\cdots}O_{water}$ bonds that they form. See Figure 3. The $[HSeO_3]$ groups are canted with respect to the direction of layer propagation, see Figure 3b, which minimizes steric repulsion between adjacent stereoactive lone pairs and allows for selenium centers on adjacent chains to be farther apart (3.5748(7) Å in $[C_6H_{14}N_2][VO(SeO_3)(HSeO_3)]_2{\cdot}2H_2O$ versus 3.4107(10) Å in **1**). The reduced steric interactions between selenium centers enable the formation of stronger $V{-}O_{trans}$ bonds in $[C_6H_{14}N_2][VO(SeO_3)(HSeO_3)]_2{\cdot}2H_2O$ (2.277(4) Å, 0.50 vu) with respect to **1** (2.688(4) Å, 0.09 vu) and result in the formation of two-dimensional layers.

The hydrogen-bonding environment around the $[2,5\text{-dmpipH}_2]^{2+}$ cation in **2** is much more isotropic with respect to $[1,4\text{-dmpipH}_2]^{2+}$ or $[dabcoH_2]^{2+}$. See Figure 5. This forces

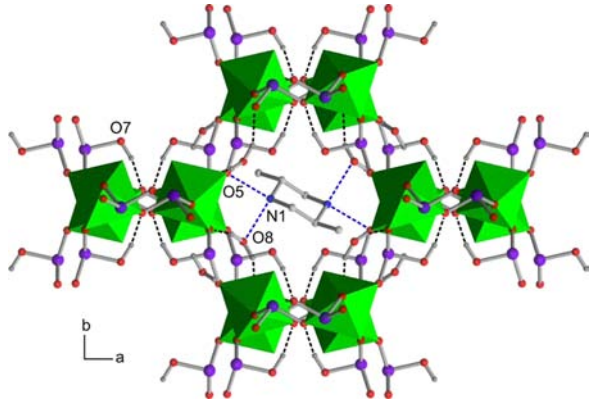

Figure 5. Hydrogen-bonding interactions, shown as dashed lines, in **2**. Green polyhedra represent $[VO_6]$, while purple, red, blue, white, and gray spheres represent selenium, oxygen, nitrogen, carbon, and hydrogen, respectively. Organic ammonium cation hydrogen atoms have been removed for clarity.

the chain SBUs to link more closely together in a three-dimensional fashion in order to satisfy the hydrogen-bonding preferences of the $[2,5\text{-dmpipH}_2]^{2+}$ cations. Small pockets exist between adjacent SBU chains in which occluded water molecules reside. No such occluded water molecules are observed in **1** because these pockets do not exist. Instead, the regions between chains are largely occupied by $[HSeO_3]$ groups and their associated stereoactive lone pairs.

The Se^{4+} stereoactive lone pairs force an 'off-center' placement of these molecules, which in turn help satisfy the

dx.doi.org/10.1021/ic3015496 | *Inorg. Chem.* 2012, 51, 11040−11048

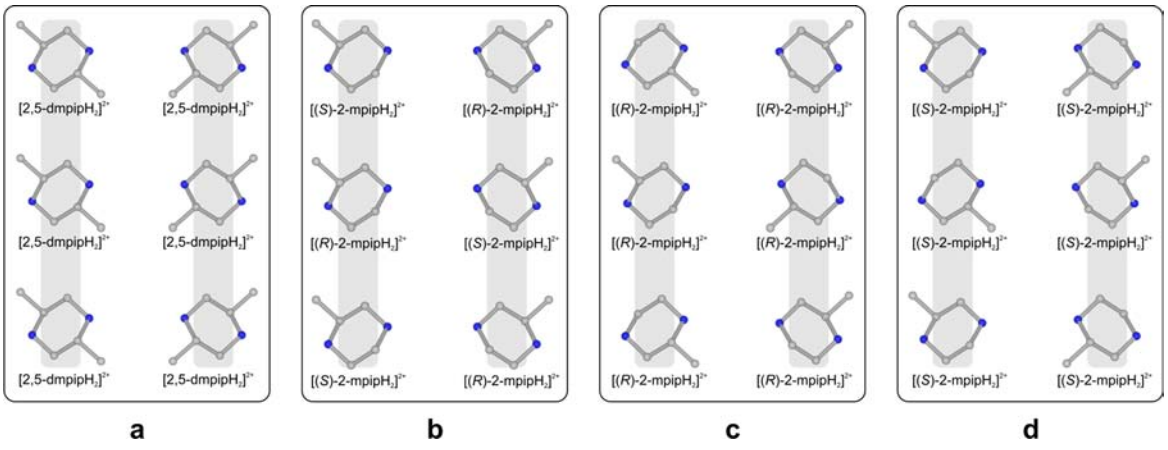

Figure 6. Organic cation orientations in (a) **2**, (b) **3**, (c) **4a**, and (d) **4b**.

hydrogen-bonding preferences of the $[2,5\text{-dmpipH}_2]^{2+}$ cations, as they are strong acceptors. A figure showing the placement of these water molecules is provided in the Supporting Information. These water molecules do not affect the orientation of the $[HSeO_3]$ groups because they accept hydrogen bonds from the $[2,5\text{-dmpipH}_2]^{2+}$ cations. Instead, the $[HSeO_3]$ groups form *intra*-SBU hydrogen bonds (O7−H1···O3). The water molecule (O8) hydrogen bonds to O2 and O6 through distances of 2.742(2) and 2.743(2) Å, respectively, while N1−H4···O5 and N1−H4···O8 bonds of 2.795(2) and 2.712(2) Å are also observed.

The one-dimensional SBU chains in $[C_4H_{12}N_2][VO(H_2O)_2(SeO_3)]_2[SO_4]$[56] and $[[VO(H_2O)_2](SeO_3)]_4{\cdot}2H_2O$[57] are unable to form higher-dimensionality structures because of the presence of two bound water molecules per vanadium center. The only $[SeO_3]$ groups in these compounds are part of the ladder-type chain backbone; no 'pendant' $[SeO_3]$ or $[HSeO_3]$ groups are available to link adjacent chains. See Figure 4d. Extensive hydrogen-bonding exists between neighboring chains, but stronger interactions are not observed. In contrast, the one-dimensional SBUs in $[C_4H_{12}N_2]_{0.5}[(VO)_2(H_2O)_2(SeO_3)_2(HSeO_3)]$ are able to form two-dimensional layers because of an additional $[HSeO_3]$ group per vanadium center that bridges between chains. See Figure 4e. Polyhedral figures of the chains and layers in $[C_4H_{12}N_2][VO(H_2O)_2(SeO_3)]_2[SO_4]$ and $[C_4H_{12}N_2]_{0.5}[(VO)_2(H_2O)_2(SeO_3)_2(HSeO_3)]$, respectively, are shown in the Supporting Information.

In an analogous fashion to **1**, the only hydrogen bond acceptors in $[C_4H_{12}N_2]_{0.5}[(VO)_2(H_2O)_2(SeO_3)_2(HSeO_3)]$ are the oxide anions within the inorganic structure. As such, *intra*-SBU hydrogen bonds are observed, which result in $[HSeO_3]$ orientations that are nearly identical to **1**. However, only a single bridging $[HSeO_3]$ group is present between adjacent vanadium centers in $[C_4H_{12}N_2]_{0.5}[(VO)_2(H_2O)_2(SeO_3)_2(HSeO_3)]$, owing to the reduced selenite content of this compound. This allows the $[HSeO_3]$ group to occupy equatorial sites on both vanadiums and enables neighboring selenium centers to be much farther apart (4.3543(11) Å) with respect to **1** (3.4107(10) Å) or $[C_6H_{14}N_2][VO(SeO_3)(HSeO_3)]_2{\cdot}2H_2O$ (3.5748(7) Å). The steric forces between nearby selenite groups that preclude layer formation in **1** (see Figure 4a) are not present in $[C_4H_{12}N_2]_{0.5}[(VO)_2(H_2O)_2(SeO_3)_2(HSeO_3)]$ and $[(VO)_2(H_2O)_2(SeO_3)_2(HSeO_3)]_n^{n-}$ layers can form.

The relative nucleophilicities of the 'vanadyl' oxide anions in these compounds are generally high, according to the bond valence sums. While these sites do not accept N−H···O hydrogen bonds, they each accept multiple C−H···O hydrogen bonds. These longer, weaker interactions[73,74] are well-known to be ubiquitous in such compounds, with recent reports in a variety of systems.[38,75] The 'vanadyl' oxygen sites in **1**, $[C_6H_{14}N_2][VO(SeO_3)(HSeO_3)]_2{\cdot}2H_2O$, and **2** each accept three C−H···O hydrogen bonds with D···A distances ranging between 3.179(8) and 3.597(8) Å, which help satisfy the underbonded 'vanadyl' oxygens.

Effects associated with amine volume do not appear to affect the dimensionality of the inorganic structures strongly. Within the set of compounds discussed here, one-dimensional chain compounds are observed for both the smallest (piperazine) amines and largest (1,4-dmpip) amine, while three-dimensional framework structures are found to include both the largest (2,5-dmpip) and smaller (2-mpip) amines. Instead, the compositions of the SBU and the interactions between the anionic and cationic components contribute most greatly to the formation of the final structures.

Understanding the formation of the three-dimensional $[VO(SeO_3)(HSeO_3)]_n^{n-}$ framework in **2** affords an opportunity for the directed synthesis of noncentrosymmetric framework compounds. Specifically, the use of chiral analogues of 2,5-dmpip would be anticipated to enforce crystallographic noncentrosymmetry, while retaining the framework structure. The well-known effect of using chiral components for the creation noncentrosymmetric products[37,68,70,76−80] has again been exploited in this work to form noncentrosymmetric analogues of compound **2**. Specifically, 2,5-dimethylpiperazine in the synthesis of **2** was replaced with either racemic or enantiomerically pure sources of 2-methylpiperazine. These reactions resulted in $[C_5H_{14}N_2][VO(SeO_3)(HSeO_3)]_2{\cdot}2H_2O$ (**3**) and a pair of enantiomers: $[(R)\text{-}C_5H_{14}N_2][VO(SeO_3)(HSeO_3)]_2{\cdot}2H_2O$ (**4a**) and $[(S)\text{-}C_5H_{14}N_2][VO(SeO_3)(HSeO_3)]_2{\cdot}2H_2O$ (**4b**).

The relative charges, pK_as, and hydrogen-bonding properties of 2,5-dmpip and 2-mpip are nearly identical, suggesting that reactions using these two amines would likely contain similar inorganic structures. Compounds **3** and **4a**/**4b** contain three-dimensional frameworks with the same connectivities as compound **2**. Packing figures for these compounds can be found in the Supporting Information. A comparison of the structures reveals that the largest differences between

dx.doi.org/10.1021/ic3015496 | *Inorg. Chem.* 2012, 51, 11040−11048

compounds are the positions of the methyl groups on the organic cations. Columns of cations that reside in adjacent channels in compounds **2**, **3**, **4a**, and **4b** are shown in Figure 6. Compound **3** contains alternating $[(S)\text{-2-mpipH}_2]^{2+}$ and $[(R)\text{-2-mpipH}_2]^{2+}$ cations. The direction of the methyl groups, both within and between columns of cations, are preserved in that they all point 'up', as shown in Figure 6b. In contrast, the directions of the methyl groups alternate in an 'up−down' fashion, both within and between columns of cations in **4a** and **4b**. See Figure 6c-d.

The orientations of the cations result in marked differences in symmetry between compounds **2**, **3**, and **4a**/**4b**. Compound **2**, which contains 2,5-dmpip, crystallizes in the centrosymmetric space group *Pbcn* (no. 60). The $[2,5\text{-dmpipH}_2]^{2+}$ cations contain an internal inversion center, and only one unique vanadium and two unique selenium sites are observed in the crystal structure. **3**, which contains racemic 2-mpip, crystallizes in the polar, achiral noncentrosymmetric space group $Pca2_1$ (no. 29, crystal class *mm*2). The $[(R)\text{-2-mpipH}_2]^{2+}$ and $[(S)\text{-2-mpipH}_2]^{2+}$ cations in **3** are related to one another through a series of glide planes,[81] which allow for the formation of a polar structure but preclude chirality. The Flack parameter for **3** refines to 0.199(11), indicating partial twinning, as discussed in the Supporting Information. Compounds **4a** and **4b**, in contrast, crystallize in the nonpolar, chiral noncentrosymmetric space group $P2_12_12$ (no. 18, crystal class 222), with Flack parameters of 0.027(11) and 0.026(12), respectively. In these structures, the complete resolution of the respective enantiomers forces the crystallization in a chiral space group. However, the presence of multiple orthogonal axes of rotation results in the loss of net polarity. This is most easily observed in the positions of the methyl groups in Figure 6. The decreased volume of 2-mpip with respect to 2,5-mpip results in small decreases of the crystallographic axes along which the channels are aligned, with distances of 12.667(5) to 12.682(2) Å for compounds **3** and **4a**/**4b** versus 12.7160(14) Å for **2**.

While **3** and **4a**/**4b** are all noncentrosymmetric, some pseudoinversion symmetry is present within the inorganic frameworks in each compound, as observed using PLATON.[82] In these three compounds, the organic cations represent the only deviations from centrosymmetry. Specifically, the pseudoinversion sites in **3** are located off-center in the $[C_5H_{14}N_2]^{2+}$ cations, while the pseudoinversion sites in **4a**/**4b** are located within the SBU chain backbones. The positions of the organic cation methyl groups in **4a**/**4b** break this pseudosymmetry. A detailed discussion of the pseudosymmetry in **3** is included in the Supporting Information. The true noncentrosymmetry in these compounds reflects the structures of their respective organic amines.

The magnitudes and directions of both component and net dipole moments were calculated[15,20,37,52] for the polar compound **3** in order to understand how component dipole moments cancel. The Hirshfeld-I scheme[49,50,83] was used to determine partial atomic charges for all atoms in **3** in order to calculate the dipole moments. The vanadium charges are 1.48 and 1.50. The selenium centers in $[SeO_3]$ groups are 1.21 and 1.23, while the Se atoms in $[HSeO_3]$ groups have slightly higher charges of 1.28 and 1.29. The V=O oxygens have charges of −0.58 and −0.62, while the V−O−Se bridging oxygen atoms have charges ranging between −0.69 and −0.76. Se−O−H oxygen atoms have charges of −0.68 and −0.69. Oxygen atoms in occluded water molecules have the most negative charges, with values of −0.98 and −1.00. A table of complete Hirshfeld-I partial atomic charges is available in the Supporting Information.

Dipole moments were calculated for each $[VO_6]$, $[SeO_3]$, and $[HSeO_3]$ group, in addition to the H_2O molecules and $[2\text{-mpipH}_2]^{2+}$ cations. See Table 2 and Figure 7. The effects of

Table 2. Calculated Dipole Moments in $[C_5H_{14}N_2][VO(SeO_3)(HSeO_3)]_2\cdot 2H_2O$ (3)

species	dipole moment (D)	species	dipole moment (D)
$V(1)O_6$	8.98	$H_2O(15)$	2.54
$V(2)O_6$	9.16	$H_2O(16)$	2.52
$Se(1)O_3$	9.35	$[2\text{-mpipH}_2]^{2+}$	2.74
$Se(2)O_3$	9.43		
$HSe(3)O_3$	9.39	$[VO(SeO_3)(HSeO_3)]_n^{n-}$	0.02
$HSe(4)O_3$	9.26	framework	
		net moment	1.06

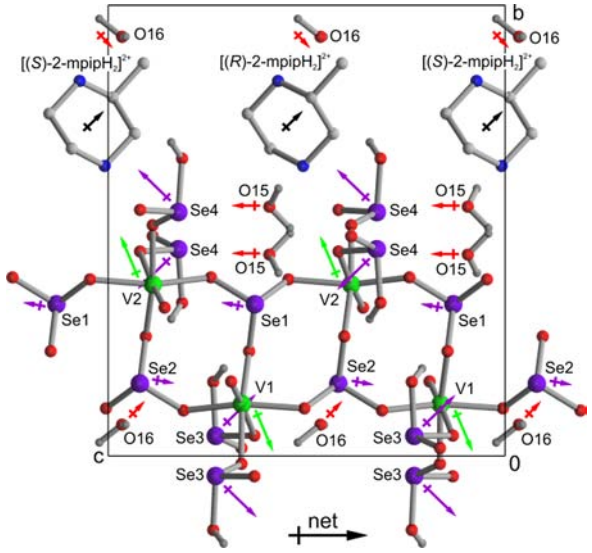

Figure 7. Ball-and-stick representation of **3**. Arrows indicate the approximate directions and magnitudes of the dipole moments for the $[VO_6]$, $[SeO_3]$, $[HSeO_3]$ polyhedra, water molecules, and the $[C_5H_{14}N_2]^{2+}$ cations. The large black arrow represents the direction of the net dipole moment for **3**. Organic ammonium cation hydrogen atoms have been removed for clarity.

pseudoinversion symmetry within the $[VO(SeO_3)(HSeO_3)]_n^{n-}$ framework are clearly evident. The component moments of the $[V(1)O_6]/[V(2)O_6]$ octahedra are essentially antialigned, as are the moments on the $[Se(1)O_3]/[Se(2)O_3]$ and $[HSe(3)O_3]/[HSe(4)O_3]$ groups and water molecules. The moments on the $[2\text{-mpipH}_2]^{2+}$ cations are not antialigned with respect to one another, and their components make the largest contributions to the net moment of the compound, which is constrained to lie along the *c*-axis.

Despite some pseudosymmetry in the inorganic framework in **3**, differences in calculated dipole moments between related sites do exist. See Table 2. The calculated dipole moments on the $[V(1)O_6]$ and $[V(2)O_6]$ octahedra and $[HSe(3)O_3]$ and $[HSe(4)O_3]$ differ by approximately 2% and 1.5%, respectively. The moments on the $[Se(1)O_3]$ and $[Se(2)O_3]$ groups, however, differ by less than 1%. The charge distribution on the $[2\text{-mpipH}_2]^{2+}$ cations is of course not symmetric, owing to the presence of the methyl group near to the N1 position. The

dx.doi.org/10.1021/ic3015496 | *Inorg. Chem.* 2012, 51, 11040−11048

asymmetry in cation charge affects the oxides to which the cations hydrogen bond.

Specifically, C2−H10···O7 and C4−H16···O1 hydrogen bonds are observed in **3**. The increased charge on C2 with respect to C4 (−0.28 versus −0.19) is reflected in the charges on O7 and O1 (−0.62 and −0.58). Additionally, the increased charge on N1 with respect to N2 (−0.49 versus 0.40) affects the charges on O9 and O6. As O1 and O7 are components in $[V(1)O_6]$ and $[V(2)O_6]$, respectively, O6 is a component in both the $[V(1)O_6]$ and $[HSe(3)O_3]$ groups, and O9 is part of $[V(2)O_6]$ and $[HSe(4)O_3]$, differences in their respective charges affect the calculated dipole moments on the $[VO_6]$ and $[HSeO_3]$ groups. A smaller difference between $[SeO_3]$ groups is observed because these groups do not directly interact with the $[2\text{-mpip}H_2]^{2+}$ cations. Figures detailing these hydrogen-bonding interactions are available in the Supporting Information.

Powder SHG measurements were performed on **3** and **4a**/**4b**. No measurable signals were observed in any compound, likely the result of absorption of the incident 1064 nm light by d−d transitions.[84] In addition, the pseudosymmetry within the inorganic frameworks in **3** and **4a**/**4b** would suggest a small activity, even in the absence of any absorption of the incident or generated light. This does not indicate crystallographic centrosymmetry. A full description of the space group assignment and pseudosymmetry in **3** is provided in the Supporting Information.

Analysis of the TGA data for compounds **2**, **3**, and **4a**/**4b** indicates that the frameworks begin to break down as the organic components decompose. Mass losses of between 24 and 26% are observed for these compounds between approximately 170 and 270 °C, which are greater than the expected mass losses from water and the amine alone (19.1% for **2** and 17.7% for **3**, **4a**, and **4b**). TGA traces for all compounds are available in the Supporting Information.

CONCLUSIONS

The compositions of the secondary building units and hydrogen-bonding interactions, both within these units and between the organic and inorganic components, provide the driving force for the evolution in dimensionality of the inorganic components in **1**, $[C_6H_{14}N_2][VO(SeO_3)(HSeO_3)]_2{\cdot}2H_2O$, and **2**. Replacing 2,5-dmpip with racemic or enantiomerically pure sources of 2-mpip results in the formation of isotopic $[VO(SeO_3)(HSeO_3)]_n^{n-}$ frameworks. However, the resulting compounds all crystallize in non-centrosymmetric space groups, owing to the lack of internal inversion symmetry in $[2\text{-mpip}H_2]^{2+}$. The use of racemic 2-mpip results in a polar achiral structure, while either (*R*)-2-mpip or (*S*)-2-mpip produces nonpolar chiral compounds.

ASSOCIATED CONTENT

Supporting Information

A full description of the space group assignment and pseudosymmetry in **3**, figures of the occluded water molecules positions in **2**, one-dimensional SBUs in **1**, $[C_6H_{14}N_2][VO(SeO_3)(HSeO_3)]_2{\cdot}2H_2O$ and **2**, pseudoinversion sites and both $|F_{obs}|$ and $|F_{obs}| - |F_{calc}|$ electron density maps in **3**, three-dimensional packing of **3** and **4a**/**4b**, calculated dipole moments for $[VO_6]$, $[SeO_3]$, and $[HSeO_3]$ groups and hydrogen bonding interactions in **3**, thermogravimetric traces for **1**, **2**, **3**, and **4a**/**4b**, the inorganic structures in $[C_4H_{12}N_2][VO(H_2O)_2(SeO_3)]_2[SO_4]$, $[[VO(H_2O)_2](SeO_3)]_4{\cdot}2H_2O$, and $[C_4H_{12}N_2]_{0.5}[(VO)_2(H_2O)_2(SeO_3)_2(HSeO_3)]$ and tables of bond valence sums for **1**, **2**, **3**, and **4a**/**4b**, iterative Hirshfeld partial atomic charges for **2** and **3**. An X-ray crystallographic information file (CIF) is available for **1**, **2**, **3**, and **4a**/**4b**. This material is available free of charge via the Internet at http://pubs.acs.org.

AUTHOR INFORMATION

Corresponding Author

*Phone: (610) 896 2949. Fax: (610) 896 4963. E-mail: anorquis@haverford.edu. http://www.haverford.edu/chem/Norquist/.

Notes

The authors declare no competing financial interest.

ACKNOWLEDGMENTS

The authors acknowledge support from the NSF (Award No. CHE-0911121), the Henry Dreyfus Teacher-Scholar Awards Program, and grants to Haverford College from the HHMI Undergraduate Science Education Program. M.Z. acknowledges support for the purchase of a diffractometer from the NSF grant 0087210, the Ohio Board of Regents grant CAP-491, and from Youngstown State University. This research used computational resources of the Extreme Science and Engineering Discovery Environment (XSEDE), which is supported by National Science Foundation grant number OCI-1053575, and the National Energy Research Scientific Computing Center (NERSC), which is supported by the Office of Science of the U.S. Department of Energy under Contract No. DE-AC02-05CH11231. P.S.H. and T.T.T. thanks the Welsh Foundation (Grant E-1457) and the Texas Center for Superconductivity for support.

REFERENCES

(1) Cheetham, A. K.; Ferey, G.; Loiseau, T. *Angew. Chem., Int. Ed.* **1999**, *38*, 3268.
(2) Ok, K. M.; Chi, E. O.; Halasyamani, P. S. *Chem. Soc. Rev.* **2006**, *35*, 710.
(3) Burton, A.; Darton, R. J.; Davis, M. E.; Hwang, S.-J.; Morris, R. E.; Ogino, I.; Zones, S. I. *J. Phys. Chem. B* **2006**, *110*, 5273.
(4) Bull, I.; Villaescusa, L. A.; Teat, S. J.; Camblor, M. A.; Wright, P. A.; Lightfoot, P.; Morris, R. E. *J. Am. Chem. Soc.* **2000**, *122*, 7128.
(5) Huang, Q.; Hwu, S.-J. *Inorg. Chem.* **2003**, *42*, 655.
(6) Yu, P.; Zhou, L.-J.; Chen, L. *J. Am. Chem. Soc.* **2012**, *134*, 2227.
(7) Kiebach, R.; Naether, C.; Peter, S. C.; Mosel, B. D.; Poettgen, R.; Bensch, W. *J. Solid State Chem.* **2006**, *179*, 3082.
(8) Ma, L.; Abney, C.; Lin, W. *Chem. Soc. Rev.* **2009**, *38*, 1248.
(9) Dang, D.; Wu, P.; He, C.; Xie, Z.; Duan, C. *J. Am. Chem. Soc.* **2010**, *132*, 14321.
(10) Yeon, J.; Kim, S.-H.; Halasyamani, P. S. *Inorg. Chem.* **2010**, *49*, 6986.
(11) Kim, S.-H.; Yeon, J.; Halasyamani, P. S. *Chem. Mater.* **2009**, *21*, 5335.
(12) Chang, H.-Y.; Kim, S.-H.; Ok, K. M.; Halasyamani, P. S. *J. Am. Chem. Soc.* **2009**, *131*, 6865.
(13) Sivakumar, T.; Chang, H. Y.; Baek, J.; Halasyamani, P. S. *Chem. Mater.* **2007**, *19*, 4710.
(14) Sambrook, T.; Smura, C. F.; Clarke, S. J.; Ok, K. M.; Halasyamani, P. S. *Inorg. Chem.* **2007**, *46*, 2571.
(15) Kim, J.-H.; Baek, J.; Halasyamani, P. S. *Chem. Mater.* **2007**, *19*, 5637.
(16) Jiang, H.-L.; Huang, S.-P.; Fan, Y.; Mao, J.-G.; Cheng, W.-D. *Chem.—Eur. J.* **2008**, *14*, 1972.
(17) Pearson, R. G. *J. Am. Chem. Soc.* **1969**, *91*, 4947.

(18) Wheeler, R. A.; Whangbo, M. H.; Hughbanks, T.; Hoffmann, R.; Burdett, J. K.; Albright, T. A. *J. Am. Chem. Soc.* **1986**, *108*, 2222.
(19) Kunz, M.; Brown, I. D. *J. Solid State Chem.* **1995**, *115*, 395.
(20) Maggard, P. A.; Nault, T. S.; Stern, C. L.; Poeppelmeier, K. R. *J. Solid State Chem.* **2003**, *175*, 27.
(21) Marvel, M. R.; Pinlac, R. A. F.; Lesage, J.; Stern, C. L.; Poeppelmeier, K. R. *Z. Anorg. Allg. Chem.* **2009**, *635*, 869.
(22) Marvel, M. R.; Lesage, J.; Baek, J.; Halasyamani, P. S.; Stern, C. L.; Poeppelmeier, K. R. *J. Am. Chem. Soc.* **2007**, *129*, 13963.
(23) Donakowski, M. D.; Gautier, R.; Yeon, J.; Moore, D. T.; Nino, J. C.; Halasyamani, P. S.; Poeppelmeier, K. R. *J. Am. Chem. Soc.* **2012**, *134*, 7679.
(24) Murugavel, R.; Choudhury, A.; Walawalkar, M. G.; Pothiraja, R.; Rao, C. N. R. *Chem. Rev.* **2008**, *108*, 3549.
(25) Parnham, E. R.; Morris, R. E. *Acc. Chem. Res.* **2007**, *40*, 1005.
(26) Cheetham, A. K.; Rao, C. N. R. *MRS Bull.* **2005**, *30*, 93.
(27) Ferey, G. *Chem. Mater.* **2001**, *13*, 3084.
(28) Harrison, W. T. A. *Curr. Opin. Solid State Mater. Sci.* **2002**, *6*, 407.
(29) Ferey, G. *J. Fluorine Chem.* **1995**, *72*, 187.
(30) Dan, M.; Udayakumar, D.; Rao, C. N. R. *Chem. Commun.* **2003**, 2212.
(31) Murugavel, R.; Walawalkar, M. G.; Dan, M.; Roesky, H. W.; Rao, C. N. R. *Acc. Chem. Res.* **2004**, *37*, 763.
(32) Chang, K. B.; Hubbard, D. J.; Zeller, M.; Schrier, J.; Norquist, A. J. *Inorg. Chem.* **2010**, *49*, 5167.
(33) Jung, K.; Kim, H.; Yun, H.; Do, J. *Z. Anorg. Allg. Chem.* **2006**, *632*, 1582.
(34) Feng, M.-L.; Mao, J.-G. *J. Solid State Chem.* **2005**, *178*, 2256.
(35) Huang, X.; Liu, Z.; Huang, C.; Shen, L.; Yan, X. *Acta Crystallogr., Sect. C: Cryst. Struct. Commun.* **2009**, *C65*, m385.
(36) Huang, X.; Liu, Z.; Huang, C.; Shen, L.; Yan, X. *Acta Crystallogr., Sect. C: Cryst. Struct. Commun.* **2009**, *C65*, m404.
(37) Glor, E. C.; Blau, S. M.; Yeon, J.; Zeller, M.; Shiv Halasyamani, P.; Schrier, J.; Norquist, A. J. *J. Solid State Chem.* **2011**, *184*, 1445.
(38) Smith, M. D.; Blau, S. M.; Chang, K. B.; Zeller, M.; Schrier, J.; Norquist, A. J. *Cryst. Growth Des.* **2011**, *11*, 4213.
(39) Gao, B.; Liu, S.; Xie, L.; Wang, X.; Zhang, C.; Sun, C.; Hu, N.; Jia, H. *J. Solid State Chem.* **2005**, *178*, 1825.
(40) Bruker AXS Inc.: Madison, WI, USA, 2009.
(41) Altomare, A.; Cascarano, G.; Giacovazzo, C.; Guagliardi, A. *J. Appl. Crystallogr.* **1993**, *26*, 343.
(42) Betteridge, P. W.; Carruthers, J. R.; Cooper, R. I.; Prout, K.; Watkin, D. J. *J. Appl. Crystallogr.* **2003**, *36*, 1487.
(43) Dowty, E. Shape Software: TN, USA, 2002.
(44) Kurtz, S. K.; Perry, T. T. *J. Appl. Phys.* **1968**, *39*, 3798.
(45) Porter, Y.; Ok, K. M.; Bhuvanesh, N. S. P.; Halasyamani, P. S. *Chem. Mater.* **2001**, *13*, 1910.
(46) Gonze, X.; Beuken, J. M.; Caracas, R.; Detraux, F.; Fuchs, M.; Rignanese, G. M.; Sindic, L.; Verstraete, M.; Zerah, G.; Jollet, F.; Torrent, M.; Roy, A.; Mikami, M.; Ghosez, P.; Raty, J. Y.; Allan, D. C. *Comput. Mater. Sci.* **2002**, *25*, 478.
(47) Gonze, X.; Amadon, B.; Anglade, P. M.; Beuken, J. M.; Bottin, F.; Boulanger, P.; Bruneval, F.; Caliste, D.; Caracas, R.; Cote, M.; Deutsch, T.; Genovese, L.; Ghosez, P.; Giantomassi, M.; Goedecker, S.; Hamann, D. R.; Hermet, P.; Jollet, F.; Jomard, G.; Leroux, S.; Mancini, M.; Mazevet, S.; Oliveira, M. J. T.; Onida, G.; Pouillon, Y.; Rangel, T.; Rignanese, G. M.; Sangalli, D.; Shaltaf, R.; Torrent, M.; Verstraete, M. J.; Zerah, G.; Zwanziger, J. W. *Comput. Phys. Commun.* **2009**, *180*, 2582.
(48) Momma, K.; Izumi, F. *J. Appl. Crystallogr.* **2008**, *41*, 653.
(49) Bultinck, P.; Van Alsenoy, C.; Ayers, P. W.; Carbo-Dorca, R. *J. Chem. Phys.* **2007**, *126*, 144111.
(50) Bultinck, P.; Ayers, P. W.; Fias, S.; Tiels, K.; Van Alsenoy, C. *Chem. Phys. Lett.* **2007**, *444*, 205.
(51) Gaigalas, G.; Froese Fischer, C. *Comput. Phys. Commun.* **1996**, *98*, 255.
(52) Izumi, H. K.; Kirsch, J. E.; Stern, C. L.; Poeppelmeier, K. R. *Inorg. Chem.* **2005**, *44*, 884.
(53) Brown, I. D.; Altermatt, D. *Acta Crystallogr., Sect. B: Struct. Sci.* **1985**, *41*, 244.
(54) Brese, N. E.; O'Keeffe, M. *Acta Crystallogr., Sect. B: Struct. Sci.* **1991**, *47*, 192.
(55) Brown, I. D. *The chemical bond in inorganic chemistry*; Oxford University Press: Oxford, 2002.
(56) Lian, Z.; Huang, C.; Zhang, H.; Yang, H.; Zhang, Y.; Yang, X. *J. Chem. Crystallogr.* **2004**, *34*, 489.
(57) Dai, Z.; Shi, Z.; Li, G.; Chen, X.; Lu, X.; Xu, Y.; Feng, S. *J. Solid State Chem.* **2003**, *172*, 205.
(58) Dai, Z.; Li, G.; Shi, Z.; Liu, X.; Feng, S. *Inorg. Chem. Commun.* **2005**, *8*, 890.
(59) Pasha, I.; Choudhury, A.; Rao, C. N. R. *Inorg. Chem.* **2003**, *42*, 409.
(60) Ayi, A. A.; Choudhury, A.; Natarajan, S.; Neeraj, S.; Rao, C. N. R. *J. Mater. Chem.* **2001**, *11*, 1181.
(61) Rao, C. N. R.; Dan, M.; Behera, J. N. *Pure Appl. Chem.* **2005**, *77*, 1655.
(62) Thomas, P. M.; Norquist, A. J.; Doran, M. B.; O'Hare, D. *J. Mater. Chem.* **2003**, *13*, 88.
(63) Doran, M. B.; Cockbain, B. E.; Norquist, A. J.; O'Hare, D. *Dalton Trans.* **2004**, 3810.
(64) Doran, M. B.; Norquist, A. J.; O'Hare, D. *Inorg. Chem.* **2003**, *42*, 6989.
(65) Norquist, A. J.; Doran, M. B.; Thomas, P. M.; O'Hare, D. *Inorg. Chem.* **2003**, *42*, 5949.
(66) Heier, K. R.; Norquist, A. J.; Wilson, C. G.; Stern, C. L.; Poeppelmeier, K. R. *Inorg. Chem.* **1998**, *37*, 76.
(67) Norquist, A. J.; Doran, M. B.; O'Hare, D. *Inorg. Chem.* **2005**, *44*, 3837.
(68) Veltman, T. R.; Stover, A. K.; Narducci Sarjeant, A.; Ok, K. M.; Halasyamani, P. S.; Norquist, A. J. *Inorg. Chem.* **2006**, *45*, 5529.
(69) Casalongue, H. S.; Choyke, S. J.; Narducci Sarjeant, A.; Schrier, J.; Norquist, A. J. *J. Solid State Chem.* **2009**, *182*, 1297.
(70) Hubbard, D. J.; Johnston, A. R.; Sanchez Casalongue, H.; Narducci Sarjeant, A.; Norquist, A. J. *Inorg. Chem.* **2008**, *47*, 8518.
(71) Kaufman, E. A.; Zeller, M.; Norquist, A. J. *Cryst. Growth Des.* **2010**, *10*, 4656.
(72) Schindler, M.; Hawthorne, F. C.; Baur, W. H. *Chem. Mater.* **2000**, *12*, 1248.
(73) Desiraju, G. R. *Chem. Commun.* **2005**, 2995.
(74) Desiraju, G. R. *Acc. Chem. Res.* **2002**, *35*, 565.
(75) Olshansky, J. H.; Blau, S. M.; Zeller, M.; Schrier, J.; Norquist, A. J. *Cryst. Growth Des.* **2011**, *11*, 3065.
(76) Gutnick, J. R.; Muller, E. A.; Narducci Sarjeant, A.; Norquist, A. J. *Inorg. Chem.* **2004**, *43*, 6528.
(77) Muller, E. A.; Cannon, R. J.; Narducci Sarjeant, A.; Ok, K. M.; Halasyamani, P. S.; Norquist, A. J. *Cryst. Growth Des.* **2005**, *5*, 1913.
(78) Choyke, S. J.; Blau, S. M.; Larner, A. A.; Narducci Sarjeant, A.; Yeon, J.; Halasyamani, P. S.; Norquist, A. J. *Inorg. Chem.* **2009**, *48*, 11277.
(79) Kepert, C. J.; Prior, T. J.; Rosseinsky, M. J. *J. Am. Chem. Soc.* **2000**, *122*, 5158.
(80) Inoue, M.; Yamase, T. *Bull. Chem. Soc. Jpn.* **1995**, *68*, 3055.
(81) Poeppelmeier, K. R. Private communication.
(82) Spek, A. L. *J. Appl. Crystallogr.* **2003**, *36*, 7.
(83) Van Damme, S.; Bultinck, P.; Fias, S. *J. Chem. Theory Comput.* **2009**, *5*, 334.
(84) Keene, T. D.; D'Alessandro, D. M.; Kramer, K. W.; Price, J. R.; Price, D. J.; Decurtins, S.; Kepert, C. J. *Inorg. Chem.* **2012**, *51*, 9192.